

## ARTICLE

# Ring-Polymer Molecular Dynamics Studies of Thermal Rate Coefficients for Reaction $F+H_2O\rightarrow HF+OH$

Jun Li\*

*School of Chemistry and Chemical Engineering, Chongqing University, Chongqing 400044, China*

(Dated: Received on August 17, 2018; Accepted on September 11, 2018)

The prototype tetra-atomic reaction  $F+H_2O\rightarrow HF+OH$  plays a significant role in both atmospheric and astronomical chemistry. In this work, thermal rate coefficients of this reaction are determined with the ring polymer molecular dynamics (RPMD) method on a full-dimensional potential energy surface (PES). This PES is the most accurate one for the title reaction, as demonstrated by the correct barrier height and reaction energy, compared to the benchmark calculations by the focal point analysis and the high accuracy extrapolated *ab initio* thermochemistry methods. The RPMD rate coefficients are in excellent agreement with those calculated by the semiclassical transition state theory and a two-dimensional master equation technique, and some experimental measurements. As has been found in many RPMD applications, quantum effects, including tunneling and zero-point energy effects, can be efficiently and effectively captured by the RPMD method. In addition, the convergence of the results with respect to the number of beads is rapid, which is also consistent with previous RPMD applications.

**Key words:** Rate coefficients, Ring polymer molecular dynamics, Quantum tunneling

## I. INTRODUCTION

The rate coefficient, usually denoted as  $k$ , is a key quantity to measure the rate of a chemical reaction in modern physical chemistry. For a reaction between two reactants, namely, bimolecular reaction, its rate coefficient is largely determined by the transition state within the framework of transition-state theory (TST). The transition state, firstly proposed by Eyring, Evans, Polanyi, and Wigner in 1930s, is an activated complex, which, once reached, will proceed to products without ever returning. Afterwards, numerous theoretical methods have been developed to predict reaction rate coefficients within the framework of transition state theory, which has become a powerful and effective tool to study chemical kinetics [1–4]. However, several issues are often blamed when the rate coefficients calculated by TST based theories are not sufficiently accurate. Firstly, the rotational and vibrational motions perpendicular to the reaction coordinate are often treated as rigid rotors and harmonic oscillators (RRHO) within TST, *i.e.* anharmonicity and coupling between these motions are generally ignored. Secondly, within the TST assumption, it is difficult to determine the multidimensional tunneling accurately, particularly in the deep tunneling regime. Thirdly, the dynamical effect such as recrossing requires

a more rigorous treatment.

According to the Born-Oppenheimer approximation, the most accurate treatment for calculating rate coefficients is to solve the nuclear Schrodinger equation on a given potential energy surface (PES), namely, the quantum mechanical (QM) approach. Although many efforts have been devoted to this field recently [5–8], and extremely accurate rate coefficients have been calculated by the QM approach for reactive systems of small number of atoms [9, 10], it is still very expensive, even impractical, to compute thermal rate coefficients accurately by Boltzmann averaging over initial reactant states for systems with four or more atoms, especially for those with two or more non-hydrogen atoms, as has been demonstrated in recent time-dependent wave packet studies on the kinetics for the complex-forming reaction  $OH+CO\rightarrow H+CO_2$  [11, 12]. Some also resort to the classical mechanism, which describes the nuclear dynamics according to the Newtonian equation. This so-called quasi-classical trajectory (QCT) method [13] is efficient with low computational cost with the dynamical effect taken into account explicitly, albeit classically. However, many important quantum effects, including tunneling, zero-point energy (ZPE) conservation, and resonances, can't be captured within the framework of the classical mechanism. Consequently, its accuracy is sometimes doubtful, especially at low temperatures and energies, when the quantum effects are significant.

Recently, the ring-polymer molecular dynamics approach (RPMD) was proposed and developed [14–17]

\* Author to whom correspondence should be addressed. E-mail: jli15@cqu.edu.cn

to provide accurate thermal rate coefficients efficiently due to the favorable scaling laws associated with classical trajectories [3]. Indeed, it has recently emerged as an efficient and reasonably accurate approach to describe quantum effects such as ZPE, anharmonicity, and tunneling, *etc.*, for calculating thermal rate coefficients. Besides, as outlined in the recent review of RPMD rate theory, several additional desirable features are expected [3]: (i) at the high temperature limit, the ring polymer collapses to a single bead, and the resulting RPMD rate coefficient becomes exact; (ii) it offers an upper bound on the RPMD rate coefficient; and (iii) the RPMD rate coefficient is independent of the definition of the dividing surface, a very promising feature as an optimal dividing surface is often very difficult to be defined in the multi-dimensional space for polyatomic reactions. Therefore, for many bimolecular reaction systems, the RPMD rate theory has been shown to be able to provide accurate rate coefficients, compared to those calculated by exact QM approach or available experiment [3, 18, 19]. As a consequence, the results calculated by the RPMD rate theory can be considered a benchmark to provide a reliable assessment of the available experiment, or theoretical results calculated by other theories [18, 19], in particular for complicated reactive systems when rigorous QM calculation is not available.

In this work, the RPMD rate theory is used to determine the rate coefficients at temperatures ranging from 200 K to 400 K for the title reaction  $F+H_2O \rightarrow HF+OH$ , which plays an important role in both atmospheric and astronomical chemistry [20, 21]. Various techniques have been employed to measure its rate coefficients [22, 23], and Atkinson *et al.* gave the recommended value as  $1.4 \times 10^{-11} \text{ cm}^3 \text{ molecule}^{-3} \text{ s}^{-1}$  independent of temperature over 240–380 K [24].

The most important factor in predicting kinetics is the barrier height due to its exponential contribution to the rate coefficients. Theoretically, due to the complicated electronic structure, the classical barrier height of the title reaction system ranges in 8.3–12.6 kcal/mol [23], 1.5 kcal/mol [25], 7.0 kcal/mol [26], 2.5 kcal/mol [27], 1.93 kcal/mol [28], at various electronic structure levels. The benchmark values are 1.534 kcal/mol by the focal point analysis (FPA) method, and 1.622 kcal/mol by the high accuracy extrapolated *ab initio* thermochemistry (HEAT) method [29]. In addition to the low reactant-like barriers, relatively deep pre-reaction complex wells [30] are found to affect the reaction dynamics and kinetics to some extent, in particular, at low collision energies or low temperatures [29, 31].

Although much has been done on the dynamics of the title system theoretically by Guo and co-workers [28, 31–40], full dimensional rigorous QM approach has not been used to compute the corresponding kinetics due to the expensive calculation cost. In this work, we use the RPMD rate theory, which can provide accurate rate coefficients with relative ease, for computing thermal

rate coefficients of the title reaction system, and for assessing available experimental or theoretical results.

## II. THEORY AND CALCULATION DETAILS

In 2012, the first full-dimensional global PES for the ground electronic state of the title reaction system was developed with more than 30,000 points calculated by the multi-reference configuration interaction (MRCI) method [28]. In order to reproduce the correct barrier height according to benchmark calculations using the focal point analysis (FPA) method, an external correlation scaling method was employed [29], and the resulting PES is able to produce the observed reactive cross sections by QCT [32] and rate coefficients by the semi-classical transition state theory and a two-dimensional master equation (SCTST/2DME) technique [29]. Besides, spin-orbit (SO) corrections were determined at the complete active space self-consistent field level [33]. Finally, the PES was fitted by using the permutation invariant polynomial neural network approach [41–43] with a total root mean square error (RMSE) of 6.8 meV, or 0.157 kcal/mol. On the PES, the barrier height is 1.798 kcal/mol, and the reaction energy is  $-17.827$  kcal/mol, which is very close to the value of  $-17.63$  kcal/mol obtained from Ruscic's Active Thermochemical Tables (ATcT) [29].

The RPMDrate code [44] is then used to compute the rate coefficients of the title reaction. The corresponding analysis of the RPMD theory for computing bimolecular rate coefficients in the gas phase and various applications have been summarized in recent review [3]. Briefly, making use of the Bennett-Chandler factorization [45], the RPMD rate coefficient depends on two factors,  $k_{\text{QTST}}(T; \xi^\ddagger)$  and  $\kappa$ , which denote the static contribution and the dynamical correction, respectively:

$$k_{\text{RPMD}} = k_{\text{QTST}}(T; \xi^\ddagger) \kappa(t \rightarrow \infty; \xi^\ddagger) \quad (1)$$

$k_{\text{QTST}}(T; \xi^\ddagger)$ , depending on the position of the dividing surface, is the rate coefficient calculated by the centroid-density quantum transition state theory (QTST). In practice, it can be estimated from the centroid potential of mean force (PMF):

$$k_{\text{QTST}}(T; \xi^\ddagger) = \frac{4\pi R_\infty^2}{\sqrt{2\pi\beta\mu_R}} e^{-\beta[W(\xi^\ddagger) - W(\xi=0)]} \quad (2)$$

where  $\mu_R$  is the reduced mass between the two reactants (in this work F and  $H_2O$ ),  $\beta = (k_B T)^{-1}$  and  $W(\xi^\ddagger) - W(\xi=0)$  denotes the PMF difference between the dividing surface ( $\xi = \xi^\ddagger$ ) and the reactant asymptote ( $\xi=0$ ), and can be obtained via umbrella integration along the dimensionless reaction coordinate ( $\xi$ ) [44].

The inclusion of the second factor  $\kappa(t \rightarrow \infty; \xi^\ddagger)$ , the transmission coefficient, can ensure that the final RPMD rate coefficient does not depend on the choice

of the dividing surface. The transmission coefficient  $\kappa$  also accounts for the recrossing effect at the top of the PMF barrier ( $\xi=\xi^\ddagger$ ). Technically, the transmission coefficient is determined by sampling ring polymer trajectories starting with their centroids pinned at  $\xi=\xi^\ddagger$ .

Within RPMD rate theory, it reduces to the classical limit when only one bead is used. In this limit, the static and dynamical components become identical to the classical TST rate coefficient and the classical transmission coefficient, respectively. Hence, these quantities establish the limit to which the quantum effects such as tunneling and ZPE can be captured with more beads. The following equation has been suggested to estimate the minimal number of beads needed to recover entire quantum effects [46]:

$$n_{\min} = \beta \hbar \omega_{\max} \quad (3)$$

where  $\omega_{\max}$  is the largest vibrational frequency of the system.

For calculating the PMF profiles, the reaction coordinate interval  $[-0.06, 1.06]$  is divided into windows with an equal size  $d\xi=0.01$ . For each sampling window, the system was firstly equilibrated for 20 ps, followed by a production run (10 ns split into 100 sampling trajectories). In this work, the Andersen thermostat is used and the ring-polymer equations of motion are integrated in Cartesian coordinates with a time step of 0.1 fs. With the inclusion of a harmonic potential  $K(\xi-\xi_i)^2$  in the system Hamiltonian, the trajectories are constrained to explore only the vicinity of  $\xi_i$ . The magnitude of the force constant  $K$  must be chosen big enough to just explore the surroundings of the window  $\xi_i$  and in the meantime small enough to allow sufficient overlapping between neighbouring  $\xi$  distributions [3]. In this work, 0.1 ( $T/K$ ) eV is used for  $K$ . Next is to determine the transmission coefficients. This is initiated by running a long mother trajectory with the ring-polymer centroid fixed at the maximum of the PMF barrier via the SHAKE algorithm [47]. Configurations are sampled once every 2 ps to serve as the initial positions for the child trajectories used to compute the flux-side correlation functions. For each initial position, 150 separate trajectories are spawned with different initial momenta sampled. These trajectories are then propagated with no constraint for 0.05 ps, which is sufficiently long to reach plateau values for the current study. These RPMD parameters have been verified for convergence, and are similar to those previously used in RPMD calculations for several thermally activated chemical reactions [3, 19, 48].

Finally, the RPMD rate coefficients are multiplied by the following electronic factor to account for the spin-orbit splitting of  $F(^2P_{1/2,3/2})$  ( $\Delta E=404 \text{ cm}^{-1}$ ).

$$\frac{Q_{\text{elec}}^{\text{TS}}}{Q_{\text{elec}}^{\text{reactants}}} = \frac{2}{4 + 2 \exp(-\beta \Delta E)} \quad (4)$$

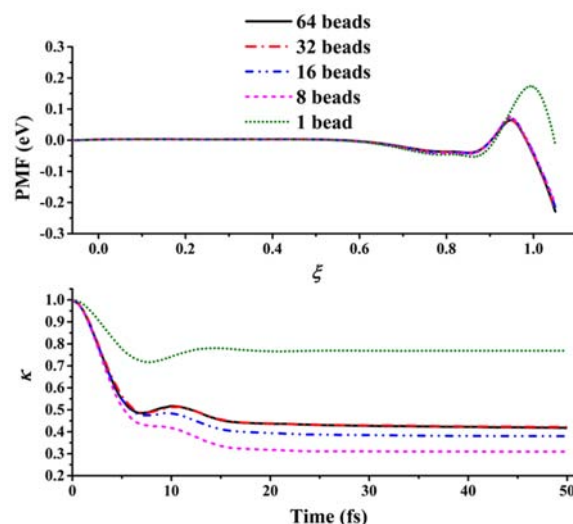


FIG. 1 Potential of mean force (in eV, relative to the reactant asymptote  $F+H_2O$ , upper panel) and transmission coefficients (lower panel) at  $T=200$  K.

### III. RESULTS AND DISCUSSION

For each temperature, 200, 300, and 400 K, we firstly perform the RPMD calculations with one bead, which provides the corresponding classical limit. Then the number of beads is increased until convergence. As shown below, most quantum effects can be captured by the first several beads. The calculation results, the PMFs along the reaction coordinate  $W(\xi)$  and the time dependence of the calculated transmission coefficients  $\kappa(t)$  with different number of beads are shown in FIGs. 1, 2, and 3, respectively, for 200, 300, and 400 K.

As shown clearly, all the PMFs at 200, 300, and 400 K possess similar features. They are flat at the reactant asymptote ( $\xi=0$ ). There exists a well around  $\xi=0.8$ , which can be attributed to the pre-reaction complex. At  $\xi=0.9-1.0$ , the PMFs go up gradually to a peak, corresponding to the barrier. Finally, they all drop down quickly, as expected due to the large exothermicity of the reaction. It can be seen that, the positions of these peaks along 1-bead PMFs are all nearly at  $\xi=1$ . As the number of beads is increased, the positions of the peaks shift to around  $\xi=0.96$  and the barrier height is lowered. They are expected since quantum effects, such as ZPE, anharmonicity, and tunneling, are well described with the inclusion of more beads. Besides, although we use as many as 32 or 64 beads to get converged results, the results calculated by 8 beads are already quite close to the converged ones. At high temperatures, the results converge even faster. From low temperatures to high temperatures, the barrier height is increased because of the decrease in entropy from reactants to the barrier, and the more significant quantum tunneling effect at low temperatures. In addition, the depth of the well is relatively deeper at low temperatures than at high

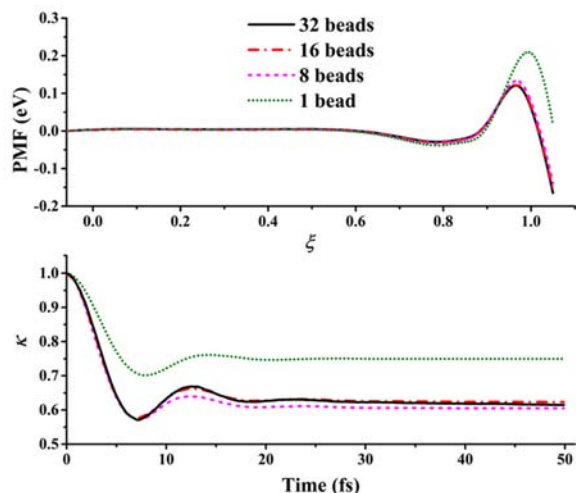


FIG. 2 Potential of mean force (in eV, relative to the reactant asymptote  $F+H_2O$ , upper panel) and transmission coefficients (lower panel) at  $T=300$  K.

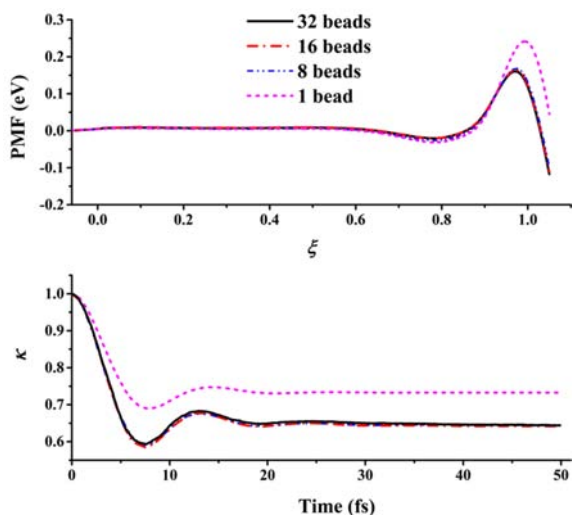


FIG. 3 Potential of mean force (in eV, relative to the reactant asymptote  $F+H_2O$ , upper panel) and transmission coefficients (lower panel) at  $T=400$  K.

temperatures. Therefore, the well would affect the kinetics and dynamics significantly at low temperatures or energies [31].

Another important factor, the transmission coefficient  $\kappa$  in Eq.(1) is also plotted along the time in the same figures. As can be seen, all the transmission coefficients show a fast initial drop for all temperatures. After oscillations,  $\kappa$  becomes flat quickly. Note that the time-dependence of  $\kappa$  is not physically meaningful, and very short time is sufficient to reach plateau values for this direct hydrogen abstraction reaction. Besides, that  $\kappa$  is small indicates significant recrossing exists even at the optimal barrier top. With the number of the beads increasing, the magnitudes of the final values of  $\kappa$  converge faster though oscillated. For instance at 300 K,  $\kappa$

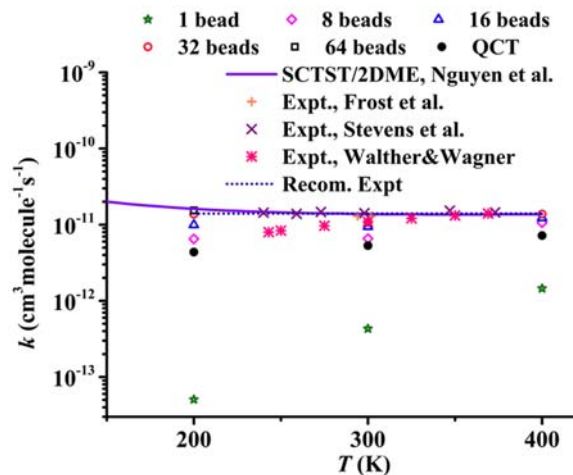


FIG. 4 Rate coefficients of the  $F+H_2O \rightarrow HF+OH$  reaction as a function of  $T$ .

is 0.75, 0.60, 0.62, and 0.61, with 1, 8, 16, and 32 beads, respectively. Note that the transmission coefficients  $\kappa$  contribute only linearly to the total RPMD rate coefficients. In addition, the transmission coefficients increase with temperature, suggesting more recrossing at low temperatures, as found in previous RPMD studies [3, 19].

The final RPMD rate coefficients are plotted as a function of  $T$  in FIG. 4, and are compared with available theoretical [29] and experimental values [22–24, 49]. It can be seen that the RPMD rate coefficients converge fast with the number of beads increasing from 1 bead to 32 beads or 64 beads for temperatures of 200, 300, and 400 K. The converged RPMD rate coefficients are in good agreement with experiment measurements and the theoretical results calculated by the SCTST/2DME technique [29]. The slightly negative temperature dependence within this temperature range is also reproduced. At 200, 300, and 400 K, the converged RPMD rate coefficients are  $1.54 \times 10^{-11}$ ,  $1.08 \times 10^{-11}$ , and  $1.38 \times 10^{-11}$   $\text{cm}^3 \text{molecule}^{-3} \text{s}^{-1}$ , respectively, compared to  $1.62 \times 10^{-11}$ ,  $1.38 \times 10^{-11}$ , and  $1.38 \times 10^{-11}$   $\text{cm}^3 \text{molecule}^{-3} \text{s}^{-1}$  determined by SCTST/2DME [29]. The largest deviation occurs at 300 K. However, the RPMD rate coefficient at 300 K agrees well with the experiment by Walther and Wagner,  $1.09 \times 10^{-11}$   $\text{cm}^3 \text{molecule}^{-3} \text{s}^{-1}$  [49]. As discussed above, RPMD method is an approximate quantum mechanical dynamics method, and can reliably capture quantum effects such as ZPE, tunneling, anharmonicity, *etc.* However, previous studies pointed out that for asymmetric reactions, like the title reaction here, the RPMD might overestimate the rate coefficients, in particular for the deep tunneling region below the crossover temperature, ca. 270 K for the title system [3, 50]. In certain cases, the RPMD is accurate even for deep tunneling region [51]. SCTST, albeit within TST framework, can provide very accurate rate coefficients since

it includes several important and advanced techniques such as non-empirical treatment of the tunneling, intrinsic anharmonicity for all vibrational motions, and coupling of the reaction coordinate to the orthogonal degrees of freedom [2]. Further rigorous QM calculations for this reaction will be very helpful to assess the two methods. Note that for clarity, the large error bounds of the observed data by Walther and Wagner are not included [49]. Nonetheless, their data are significantly smaller than other two measurements and the computational values, in particular at temperatures below 300 K.

Previously, the thermal rate coefficients for the title reaction were also determined by the QCT method [29]. The results are included in FIG. 4 for comparison. It can be seen that QCT underestimates rate coefficients of the title reaction within 200–400 K, and the underestimation becomes more significant when the temperature is decreased. This is apparently due to the fact that the QCT method lacks of quantum effects, such as tunneling and ZPE effects. As has been reported in our previous work, the SCTST calculated tunneling corrections are 3.5 at 200 K, 2.0 at 300 K, and 1.5 at 400 K, respectively. With these tunneling corrections, the QCT calculated rate coefficients are quite close to experiment (within 20%) [29].

#### IV. CONCLUSION

In this work, thermal rate coefficients at 200, 300, and 400 K for an important reaction  $F+H_2O$ , which is relevant to both atmospheric and astronomical chemistry, have been determined with the full dimensional approximate QM method, RPMD. The agreement with some experimental results and previous SCTST/2DME predicted values is excellent. In particular, it reproduces the slightly negative temperature dependence of the rate coefficients in the range of 200 K to 400 K, apparently due to tunneling. The current study provides another example not only to demonstrate the high credibility of the RPMD method for calculating thermal coefficients of polyatomic reactions, but also to assess the SCTST method and the available measurements. There are still some discrepancies between RPMD and SCTST and experiment results, albeit small and within the error bounds of experiment. Further rigorous QM calculations for this reaction system will be very helpful to resolve this issue.

#### V. ACKNOWLEDGEMENTS

This work was supported by the National Natural Science Foundation of China (No.21573027).

- [1] A. Fernández-Ramos, J. A. Miller, S. J. Klippenstein, and D. G. Truhlar, *Chem. Rev.* **106**, 4518 (2006).
- [2] T. L. Nguyen, J. F. Stanton, and J. R. Barker, *Chem. Phys. Lett.* **499**, 9 (2010).
- [3] Y. V. Suleimanov, F. J. Aoiz, and H. Guo, *J. Phys. Chem. A* **120**, 8488 (2016).
- [4] S. J. Klippenstein, *Proc. Combust. Inst.* **36**, 77 (2017).
- [5] S. C. Althorpe and D. C. Clary, *Annu. Rev. Phys. Chem.* **54**, 493 (2003).
- [6] J. M. Bowman, G. Czako, and B. N. Fu, *Phys. Chem. Chem. Phys.* **13**, 8094 (2011).
- [7] J. Li, B. Jiang, H. W. Song, J. Y. Ma, B. Zhao, R. Dawes, and H. Guo, *J. Phys. Chem. A* **119**, 4667 (2015).
- [8] D. H. Zhang and H. Guo, *Annu. Rev. Phys. Chem.* **67**, 135 (2016).
- [9] T. Wu, H. J. Werner, and U. Manthe, *Science* **306**, 2227 (2004).
- [10] C. L. Xiao, X. Xu, S. Liu, T. Wang, W. R. Dong, T. G. Yang, Z. G. Sun, D. X. Dai, X. Xu, D. H. Zhang, and X. M. Yang, *Science* **333**, 440 (2011).
- [11] J. Li, J. Chen, D. H. Zhang, and H. Guo, *J. Chem. Phys.* **140**, 044327 (2014).
- [12] J. Y. Ma, J. Li, and H. Guo, *J. Phys. Chem. Lett.* **3**, 2482 (2012).
- [13] X. C. Hu, W. L. Hase, and T. Pirraglia, *J. Comp. Chem.* **12**, 1014 (1991).
- [14] I. R. Craig and D. E. Manolopoulos, *J. Chem. Phys.* **122**, 084106 (2005).
- [15] I. R. Craig and D. E. Manolopoulos, *J. Chem. Phys.* **123**, 034102 (2005).
- [16] R. Collepardo-Guevara, Y. V. Suleimanov, and D. E. Manolopoulos, *J. Chem. Phys.* **130**, 174713 (2009).
- [17] Y. V. Suleimanov, R. Collepardo-Guevara, and D. E. Manolopoulos, *J. Chem. Phys.* **134**, 044131 (2011).
- [18] J. X. Zuo, C. J. Xie, H. Guo, and D. Q. Xie, *J. Phys. Chem. Lett.* **8**, 3392 (2017).
- [19] J. F. Castillo and Y. V. Suleimanov, *Phys. Chem. Chem. Phys.* **19**, 29170 (2017).
- [20] P. Ricaud and F. Lefèvre, *Fluorine and the Environment*, Vol.1. A. Tressaud Ed., Amsterdam: Elsevier, (2006).
- [21] D. A. Neufeld, J. Zmuidzinas, P. Schilke, and T. G. Phillips, *Astrophys. J.* **488**, L141 (1997).
- [22] R. J. Frost, D. S. Green, M. K. Osborn, and I. W. M. Smith, *Int. J. Chem. Kinet.* **18**, 885 (1986).
- [23] P. S. Stevens, W. H. Brune, and J. G. Anderson, *J. Phys. Chem.* **93**, 4068 (1989).
- [24] R. Atkinson, D. L. Baulch, R. A. Cox, J. N. Crowley, R. F. Hampson, R. G. Hynes, M. E. Jenkin, M. J. Rossi, and J. Troe, *Atmos. Chem. Phys.* **7**, 981 (2007).
- [25] Y. Ishikawa, T. Nakajima, T. Yanai, and K. Hirao, *Chem. Phys. Lett.* **363**, 458 (2002).
- [26] M. P. Deskevich, D. J. Nesbitt, and H. J. Werner, *J. Chem. Phys.* **120**, 7281 (2004).
- [27] G. L. Li, L. Q. Zhou, Q. S. Li, Y. M. Xie, and H. F. Schaefer III, *Phys. Chem. Chem. Phys.* **14**, 10891 (2012).
- [28] J. Li, R. Dawes, and H. Guo, *J. Chem. Phys.* **137**, 094304 (2012).
- [29] T. L. Nguyen, J. Li, R. Dawes, J. F. Stanton, and H. Guo, *J. Phys. Chem. A* **117**, 8864 (2013).

- [30] J. Li, Y. L. Li, and H. Guo, *J. Chem. Phys.* **138**, 141102 (2013).
- [31] J. Li, B. Jiang, and H. Guo, *Chem. Sci.* **4**, 629 (2013).
- [32] J. Li and H. Guo, *Chin. J. Chem. Phys.* **26**, 627 (2013).
- [33] J. Li, B. Jiang, and H. Guo, *J. Chem. Phys.* **138**, 074309 (2013).
- [34] J. Li, B. Jiang, and H. Guo, *J. Am. Chem. Soc.* **135**, 982 (2013).
- [35] B. Jiang and H. Guo, *J. Am. Chem. Soc.* **135**, 15251 (2013).
- [36] B. Zhao and H. Guo, *J. Phys. Chem. Lett.* **6**, 676 (2015).
- [37] H. W. Song, J. Li, and H. Guo, *J. Chem. Phys.* **141**, 164316 (2014).
- [38] H. W. Song and H. Guo, *J. Chem. Phys.* **142**, 174309 (2015).
- [39] R. Otto, J. Y. Ma, A. W. Ray, J. S. Daluz, J. Li, H. Guo, and R. E. Continetti, *Science* **343**, 396 (2014).
- [40] A. W. Ray, J. Y. Ma, R. Otto, J. Li, H. Guo, and R. E. Continetti, *Chem. Sci.* **8**, 7821 (2017).
- [41] B. Jiang and H. Guo, *J. Chem. Phys.* **139**, 054112 (2013).
- [42] J. Li, B. Jiang, and H. Guo, *J. Chem. Phys.* **139**, 204103 (2013).
- [43] B. Jiang, J. Li, and H. Guo, *Int. Rev. Phys. Chem.* **35**, 479 (2016).
- [44] Y. V. Suleimanov, J. W. Allen, and W. H. Green, *Comput. Phys. Commun.* **184**, 833 (2013).
- [45] D. Chandler, *J. Chem. Phys.* **68**, 2959 (1978).
- [46] T. E. Markland and D. E. Manolopoulos, *J. Chem. Phys.* **129**, 024105 (2008).
- [47] J. P. Ryckaert, G. Ciccotti, and H. J. C. Berendsen, *J. Comput. Phys.* **23**, 327 (1977).
- [48] Y. L. Li, Y. V. Suleimanov, J. Li, W. H. Green, and H. Guo, *J. Chem. Phys.* **138**, 094307 (2013).
- [49] C. D. Walther and H. G. Wagner, *Ber. Bunsenger. Phys. Chem.* **87**, 403 (1983).
- [50] J. O. Richardson and S. C. Althorpe, *J. Chem. Phys.* **131**, 214106 (2009).
- [51] Y. L. Li, Y. V. Suleimanov, M. H. Yang, W. H. Green, and H. Guo, *J. Phys. Chem. Lett.* **4**, 48 (2013).